LASER HEATING AND SUBLIMATION OF CARBON PARTICLES IN A FLAME

V. S. Burakov, N. G. Kondrashov,
A. A. Stavrov, and I. S. Zakharova

UDC 621:537.517.9

The problem of the nonstationary thermal destruction of a particle is solved. The results of the calculations are compared with experimental data.

The passage of laser radiation through a flame is accompanied by an increase in its emissivity [1]. At medium powers a large part of the radiation energy absorbed by the particles goes toward heating, and the sublimation is only slight, in which case the duration of emission is quite long. At high values of the peak power of the laser radiation particles are destroyed (sublimation) and the duration of emission is short. As the power of the single pulse increases, the maximum of the laser radiation scattered by the particles is shifted toward the beginning of the pulse.

We will investigate the heating and destruction of particles in a flame by laser radiation in the context of the nonstationary theory of heat conduction in condensed matter.

It is known that the use of the heat-conduction equation for studying the interaction of laser radiation and a nontransparent particle is a good approximation to reality in the region of moderate energy flux densities ($\lesssim 10^{12}$ W/m^2), where the density of the evaporated material is low and the particle surface temperature is considerably lower than the critical value [2-4]. On transition to higher power densities (kG $\gtrsim 10^{12}$ W/m^2) a gasdynamic particle degradation mechanism is observed [4].

In [1] the system was assumed to be monodisperse and a carbon particle concentration of approximately $2 \cdot 10^{18}$ m^{-3} was obtained; in this case the most probable particle diameter was about 18 nm, and the half-width of the particle size distribution function was of the order of 10 nm. Under these conditions the particles do not interact ($\Delta l \approx 10^3$ nm, i.e., $\Delta l > 1.5d$) and it is possible to consider the heating and sublimation of an individual particle in equilibrium with the surrounding infinite gas medium up to the initial instant of time (t = 0), before the radiation source is switched on [5].

It is justifiable to adopt a phenomenological approach to the analysis of the heat- and mass-transfer processes of a carbon particle (porous body) despite its small linear dimensions: the mean free path of the phonons is limited owing to the presence of amorphous structures and is a quantity on the order of several interatomic spacings (about 1 nm) [6]. It is possible to neglect the heat losses due to free convection in view of the small linear dimensions of the particle and, at the radiation flux densities in question (10^9-10^{12} W/m^2), the absorption of radiation in the air and vapor. In fact, significant absorption in the graphite vapor starts at a flux density of about 10^{14} W/m^2 and a pulse length of approximately 10^{-6} sec, when the vapor temperature at the interface with the condensed body reaches $2 \cdot 10^4$°K [4].

Under the influence of monochromatic radiation the particle releases energy to the ambient medium by forced convection, after which evaporative heat transfer may become important.

The process of particle heating and vaporization is described by the boundary-value problem for the heat-conduction equation

---

Institute of Physics, Academy of Sciences of the Belorussian SSR, Minsk. Translated from Inzhenerno-Fizicheskii Zhurnal, Vol. 32, No. 5, pp. 895-904, May, 1977. Original article submitted May 27, 1976.

$$c(T)\rho(T)\frac{\partial T(r,t)}{\partial t}=\frac{1}{r^2}\frac{\partial}{\partial r}\left(r^2\lambda(T)\frac{\partial T(r,t)}{\partial r}\right), \tag{1}$$

$$0<r<R(t),\ t>0,$$

$$T(r,0)=T_0, \tag{2}$$

$$\lim_{r\to 0} r^2\lambda(T)\frac{\partial T}{\partial r}=0, \tag{3}$$

$$-\lambda(T)\frac{\partial T(r,t)}{\partial r}\Big|_{r=R(t)}+kG(t)=G_s. \tag{4}$$

The quantity G_S is composed of the heat conduction, evaporation, and radiation losses, i.e.,

$$G_s=\alpha(T(R(t),t)-T_m)-\rho(T)L(T)\left(\frac{dR(t)}{dt}-\frac{dR(0)}{dt}\right)+\varepsilon\sigma(T^4(R(t),t)-T_m^4). \tag{5}$$

The temperature dependences of the thermophysical constants are approximated by the relations [8-11]

$$c(T)=(2.01\cdot 10^3+0.09T-2.93\cdot 10^8T^{-2})\ \text{J/(kg}\cdot\text{deg)},$$

$$1500\ ^\circ\text{K}\leqslant T<3000\ ^\circ\text{K},$$

$$c(T)=1.92\cdot 10^3+0.10T,\ 3000\ ^\circ\text{K}<T<5000\ ^\circ\text{K},$$

$$c(T)=2.44\cdot 10^3,\ T>5000\ ^\circ\text{K};$$

$$\rho(T)=\frac{2.1\cdot 10^3}{1+6.75\cdot 10^{-6}T}\ \text{kg/m}^3;$$

$$\lambda(T)=(2.38-0.51\cdot 10^{-3}T)\ \text{W/(m}\cdot\text{deg)},1500\ ^\circ\text{K}\leqslant T<3000\ ^\circ\text{K},$$

$$\lambda(T)=1.38-0.18\cdot 10^{-3}T,\ 3000\ ^\circ\text{K}<T<5000\ ^\circ\text{K},$$

$$\lambda(T)=0.50,\ T>5000\ ^\circ\text{K};$$

$$L(T)=(6.03\cdot 10^7-3.78\cdot 10^2T)\ \text{J/kg},\ 1500\ ^\circ\text{K}\leqslant T<3000\ ^\circ\text{K},$$

$$L(T)=6.06\cdot 10^7-4.83\cdot 10^2T,\ 3000\ ^\circ\text{K}<T<5000\ ^\circ\text{K},$$

$$L(T)=4.86\cdot 10^7-5.11\cdot 10^2T,\ T>5000\ ^\circ\text{K};\ \varepsilon=0.99.$$

The heat-transfer coefficient characterizing heat transfer from the particle to the ambient medium is given by [7, 12]

$$\alpha=\frac{\text{Nu}\lambda_m}{R_0}. \tag{6}$$

When the integral heat transfer from the entire surface of the particle is taken into account, Nu is closely approximated by the empirical expression $\text{Nu}=0.84(\text{Re})^{1/2}$, where $\text{Re}=R_0U/\nu$ (λ_m and ν are determined with allowance for their temperature dependence [13]).

The dimensionless absorption coefficient for the particles was calculated from the expression [14]

$$k=k(n_1,\chi,\ R(t),\ \tilde{\lambda})=\frac{24n_1\chi}{(2-n_1^2-\chi^2)^2+(2n_1\chi)^2}\rho_1,\quad \rho_1=\frac{2\pi R}{\tilde{\lambda}}. \tag{7}$$

In our case $\rho_1 \ll 1$, the particles only weakly scatter and almost exclusively absorb the radiation. The values of n_1 and χ for carbon were found from the simplified dispersion relations (for given $\tilde{\lambda}$) $2n_1\chi=0.8+3.1\tilde{\lambda}$, $n_1^2-\chi^2=2.63\tilde{\lambda}^{0.1}$ ($0.5\ \mu<\tilde{\lambda}<6\ \mu$), and differ

by not more than 5% from the exact values calculated from more complex relations [15]. The absorptivity of carbon decreases slightly (about 20%) as the particle is heated from the initial temperature (1500°K) to the sublimation temperature [16].

We introduce the equation of evaporation kinetics [17]

$$\frac{dR(t)}{dt} = -\bar{c}\left(\frac{3}{4\pi}\right)^{1/3}\exp\left[-\frac{L(T)A}{R_g T(R(t),\ t)}\right],\quad R(0) = R_0. \tag{8}$$

Equation (8) does not take into account the effect of condensation on the velocity of the evaporation front [4, 18]. The value of $\bar{c}$ was calculated from the elastic constant matrix for carbon [6, 19]. The variation of the radiation flux density with time was determined with reference to the pulse oscillogram [1]:

$$G(t) = 3.79G_0\left\{1-\exp\left[-\left(\frac{t}{a_0}+b_0\right)^{6.5}\right]\right\}\exp\left[-\left(\frac{t}{a_0}+b_0\right)^{1.5}\right],$$
$$0 \leqslant t \leqslant 5.5\cdot 10^{-8}\ \text{sec}; \tag{9}$$
$$G(t) \equiv 0,\ t > 5.5\cdot 10^{-8}\ \text{sec};$$

where $a_0 = 2.62\cdot 10^{-8}$ sec and $b_0 = 0.4$.

In the variables φ, τ, Θ, and $\bar{R}$, Eqs. (1)-(9) may be written in the form

$$\frac{\partial\Theta(\varphi,\tau)}{\partial\tau} = \frac{1}{a(\Theta_0)c(\Theta)\rho(\Theta)\bar{R}^2\varphi^2}\cdot\frac{\partial}{\partial\varphi}\left(\varphi^2\lambda(\Theta)\frac{\partial\Theta(\varphi,\tau)}{\partial\varphi}\right)$$
$$+\frac{\varphi}{\bar{R}}\cdot\frac{d\bar{R}(\tau)}{d\tau}\cdot\frac{\partial\Theta(\varphi,\tau)}{\partial\varphi},\quad 0<\varphi<1,\ \tau>0; \tag{10}$$

$$\Theta(\varphi, 0) = \Theta_0, \tag{11}$$

$$|\Theta(0,\tau)| < \infty, \tag{12}$$

$$-\frac{\partial\Theta(\varphi,\tau)}{\partial\varphi}\Big|_{\varphi=1} + \frac{k(\bar{R})R_0}{T^0}\bar{R}(\tau)\frac{G(\tau)}{\lambda(\Theta)} = \frac{\alpha R_0\bar{R}(\tau)}{\lambda(\Theta)}$$

$$\times[\Theta(\bar{R}(\tau),\tau)-\Theta_m] + \frac{\varepsilon\sigma R_0(T^0)^3\bar{R}(\tau)}{\lambda(\Theta)}[\Theta^4(\bar{R}(\tau),\tau)-\Theta_m^4] - \frac{a(\Theta_0)}{T^0}\cdot\frac{L(\Theta)\rho(\Theta)}{\lambda(\Theta)}\bar{R}(\tau)\left(\frac{d\bar{R}(\tau)}{d\tau}-\frac{d\bar{R}(0)}{d\tau}\right), \tag{13}$$

$$\frac{d\bar{R}(\tau)}{d\tau} = -\frac{\bar{c}R_0}{a(\Theta_0)}\left(\frac{3}{4\pi}\right)^{1/3}\exp\left[-\frac{A}{R_g T^0}\cdot\frac{L(\Theta(\bar{R}(\tau),\tau))}{\Theta(\bar{R}(\tau),\ \tau)}\right],\quad \bar{R}(0) = 1; \tag{14}$$

$$\alpha = 0.84\lambda_m\left(\frac{U}{R_0\nu}\right)^{1/2}, \tag{15}$$

$$k = k_0\bar{R} = \frac{48\pi n_1\chi R_0}{\tilde{\lambda}[(2+n_1^2-\chi^2)^2+(2n_1\chi)^2]}\bar{R}(\tau), \tag{16}$$

$$G(\tau) = G_0\left\{1-\exp\left[-\left(\frac{R_0^2\tau}{a_0 a(\Theta_0)}+b_0\right)^{6.5}\right]\right\}\exp\left[-\left(\frac{R_0^2\tau}{a_0 a(\Theta_0)}+b_0\right)^{1.5}\right],$$
$$0 \leqslant \tau \leqslant \frac{5.5\cdot 10^{-8}a(\Theta_0)}{R_0^2}; \tag{17}$$

$$G(\tau) \equiv 0,\ \tau > \frac{5.5\cdot 10^{-8}a(\Theta_0)}{R_0^2}.$$

In order to obtain at the boundary points an approximation of the second order of accuracy in the space variables, we replace boundary condition (13) with the auxiliary boundary condition obtained by combining (13) and (10) with $\varphi = 1$ [20]:

$$\frac{\partial\Theta}{\partial\tau} = \frac{\lambda(\Theta)}{a(\Theta_0)c(\Theta)\rho(\Theta)}\left\{\frac{2}{h_\varphi\bar{R}}\left[\frac{k(\bar{R})R_0}{T^0\lambda(\Theta)}G(\tau)\right.\right.$$
$$-\frac{\alpha R_0}{\lambda(\Theta)}(\Theta(\bar{R},\tau)-\Theta_m)-\frac{\varepsilon\sigma R_0(T^0)^3}{\lambda(\Theta)}(\Theta^4(\bar{R},\tau)-\Theta_m^4)$$
$$+\frac{a(\Theta_0)}{T^0}\cdot\frac{\rho(\Theta)L(\Theta)}{\lambda(\Theta)}\left(\frac{d\bar{R}(\tau)}{d\tau}-\frac{d\bar{R}(0)}{d\tau}\right)$$
$$\left.-\frac{2\bar{\varphi}^2}{h_\varphi\varphi^2\bar{R}^2}\cdot\frac{\partial\Theta}{\partial\varphi}+\frac{1}{\lambda(\Theta)\bar{R}^2}\cdot\frac{\partial\lambda(\Theta)}{\partial\Theta}\left(\frac{\partial\Theta}{\partial\varphi}\right)^2\right\}+\frac{\varphi}{\bar{R}}\cdot\frac{\partial\bar{R}}{\partial\tau}\cdot\frac{\partial\Theta}{\partial\varphi}, \tag{18}$$

$$\bar{\varphi}^2 = \varphi(\varphi - h_\varphi).$$

In order to find the approximate solution of boundary-value problem (10)-(12), (18), (14)-(17), we constructed an economical, absolutely stable iteration difference scheme on a space–time network $\{\varphi_n = (n+1)h_\varphi,\ h_\varphi = 1/(N+1),\ n=0, 1, \ldots, N;\ \tau_j = j\Delta\tau\}$ [21, 22]:

$$\delta_\tau\Theta_n^{j(s+1)} = \frac{1}{a(\Theta_0)c_n^{j(s)}\rho_n^{j(s)}(\bar{R}^2)^{j(s+1)}\varphi_n^2}(\bar{\varphi}^2\bar{\lambda}_n^{(s)}\Theta_{\bar{\varphi}}^{j(s+1)})_{\varphi,n}$$
$$+\frac{\varphi_n\bar{R}^{1j(s+1)}}{\bar{R}^{j(s+1)}}\Theta_{\bar{\varphi},n}^{j(s+1)},\quad T_{\bar{\varphi},0}\equiv 0;\ n=0,\ 1,\ \ldots,\ N-1;\ j=1,2,\ldots; \tag{19}$$

$$\delta_\tau\Theta_N^{j(s+1)} = \frac{\lambda_N^{j(s)}}{a(\Theta_0)c_N^{j(s)}\rho_N^{j(s)}}\left\{\frac{2}{h_\varphi\bar{R}^{j(s+1)}}\left[\frac{k^{j(s+1)}R_0}{T^0\lambda_N^{j(s)}}G^{j(s+1)}\right.\right.$$
$$-\frac{\alpha R_0}{\lambda_N^{j(s)}}(\Theta_N^{j(s)}-\Theta_m)-\frac{\varepsilon\sigma R_0(T^0)^3}{\lambda_N^{j(s)}}((\Theta^4)_N^{j(s+1)}-\Theta_m^4)$$
$$\left.+\frac{a(\Theta_0)}{T^0}\cdot\frac{L_N^{j(s)}\rho_N^{j(s)}}{\lambda_N^{j(s)}}(\bar{R}^{1j(s+1)}-\bar{R}^{10})\right]-\frac{2\bar{\varphi}_N^2}{h_\varphi(\bar{R}^2)^{j(s+1)}\varphi_N^2}\Theta_{\bar{\varphi},N}^{j(s+1)}$$
$$\left.+\frac{1}{(\bar{R}^2)^{j(s+1)}\lambda_N^{j(s)}}\left(\frac{\partial\lambda(\Theta)}{\partial\Theta}\right)_N^{j(s)}(\Theta_{\bar{\varphi},N}^{j(s+1)})^2\right\}+\frac{\varphi_N\bar{R}^{1j(s+1)}}{\bar{R}^{j(s+1)}}\Theta_{\bar{\varphi},N}^{j(s+1)},\ j=1,2,\ \ldots; \tag{20}$$

$$\bar{R}^{j(s+1)} = \bar{R}^{j-1} + \Delta\tau\bar{R}^{1j(s+1)},\ \bar{R}^0 = 1; \tag{21}$$

$$\bar{R}^{1j(s+1)} = -\frac{\bar{c}R_0}{a(\Theta_0)}\left(\frac{3}{4\pi}\right)^{1/3}\exp\left(-\frac{A}{R_gT^0}\cdot\frac{L_N^{j(s)}}{\Theta_N^{j(s)}}\right), \tag{22}$$

$$\Theta_n^0 = \Theta_0,\quad n=0,\ 1,\ \ldots,\ N. \tag{23}$$

A linearized variant of boundary condition (19) can be obtained by means of the approximation [23]

$$(\Theta^4)_N^{j(s+1)} \simeq (\Theta^4)_N^{j-1} + 4(\Theta^3)_N^{j-1}(\Theta_N^{j(s+1)} - \Theta_N^{j-1}),$$
$$(\Theta_{\bar{\varphi},N}^{j(s+1)})^2 \simeq \Theta_{\bar{\varphi},N}^{j(s)}\Theta_{\bar{\varphi},N}^{j(s+1)}.$$

The piecewise-continuous functions $c(\Theta)$, $\rho(\Theta)$, $\lambda(\Theta)$, $d\lambda(\Theta)/d\Theta$, and $L(\Theta)$ at temperatures equal to 3000 and 5000°K were joined by means of polynomials in such a way that at these points the functions and their first and second derivatives were continuous [24].

At each iteration, system of equations (19)-(23) is solved by the sweep method [21]. The iteration cycle is continued until the solution is obtained with the required accuracy.

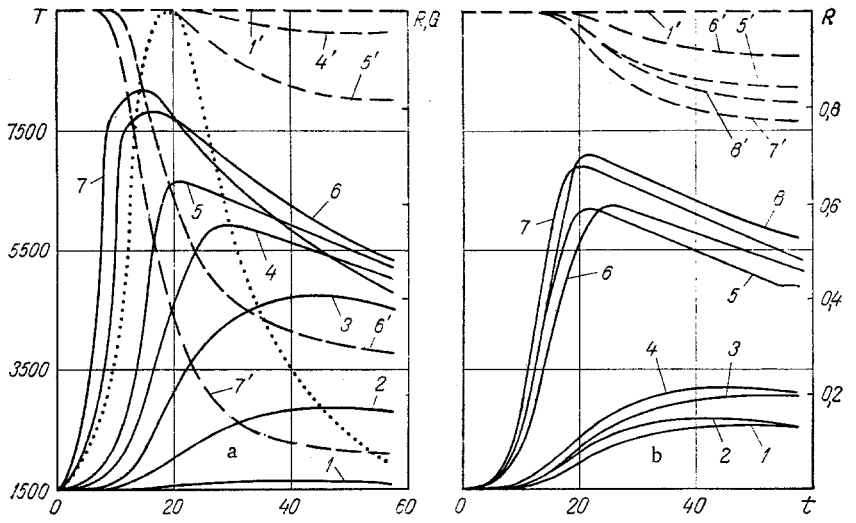

Fig. 1. Change in particle temperature and radius (continuous and dashed curves, respectively) during pulse generation (dotted curve) as a function of the laser radiation flux G_0; T, °K; t, nsec; R, G, rel. units: a) R_0 = 9 nm; $\tilde{\lambda}$ = 694.3 nm; G_0 = $1\cdot10^9$ (1, 1'), $1\cdot10^{10}$ (2, 1'), $2.5\cdot10^{10}$ (3, 1'), $5\cdot10^{10}$ (4, 4'), $1\cdot10^{11}$ (5, 5'), $5\cdot10^{11}$ (6, 6'), $1\cdot10^{12}$ (7, 7') W/m²; b) R_0 = 5 (2, 5, 1', 5'), 15 (3, 8, 1', 8') nm, $\tilde{\lambda}$ = 694.3 nm; $\tilde{\lambda}$ = 530 (4, 7, 1', 7'), 1060 (1, 6, 1', 6') nm, R_0 = 9 nm; G_0 = $1\cdot10^{10}$ (1-4, 1'), $1\cdot10^{11}$ (5-8, 5'-8') W/m².

The solution of boundary-value problem (1)-(9) exists and is unique and the approximate solution of the difference problem (19)-(23) converges to the solution of (1)-(9) at the rate $O(\Delta\tau+h_\varphi^2)$[25, 22].

Equations (19)-(23) were solved for the following parameters: Θ_0 = 1.5 (T^0 = 10^3 °K); Θ_n = 1.5; $a(\Theta_0)$ = $0.387\cdot10^{-6}$ m²/sec; U = 10 m/sec; λ_m = 0.718 W/(m·deg); ν = $2.65\cdot10^{-3}$ m²/sec; $\bar{c}$ = $2.52\cdot10^3$ m/sec; R_g = 8317 J/(deg·kmole); A = 12.011 kg/kmole); σ = $5.6696\cdot10^{-8}$ W/(m²·deg⁴); $\tilde{\lambda}$ = 530 and 694.3 nm, 1060 nm; R_0 = 5, 9, and 15 nm; G_0 = (10^9, 10^{10}, $2.5\cdot10^{10}$, $5\cdot10^{10}$, 10^{11}, $5\cdot10^{11}$, 10^{12}) W/m²; h_φ = $4\cdot10^{-2}$ (N = 24); and $\Delta\tau$ = $2\cdot10^{-3}$.

We determined the particle temperature, the variation of the particle radius with time, the evaporation rate, the radial temperature distribution, and the time dependence of the radial temperature gradient.

Figure 1a shows the variation of the surface temperature and radius of a particle with R_0 = 9 nm during the laser pulse ($\tilde{\lambda}$ = 694.3 nm) for various incident radiation fluxes. At $G_0 < 5\cdot10^{10}$ W/m² (curves 1-3) the particle is heated without being subsequently destroyed (curve 1'); in this case the heating dynamics are determined by the amount of radiation ab-

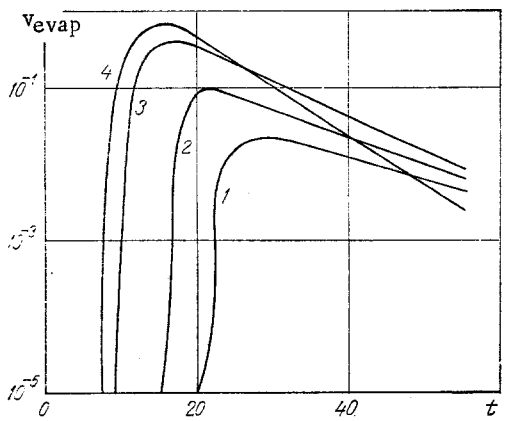

Fig. 2. Time dependence of particle evaporation rate for various laser fluxes G_0: R_0 = 9 nm; $\tilde{\lambda}$ = 694.3 nm; G_0 = $5\cdot10^{10}$ (1), $1\cdot10^{11}$ (2), $5\cdot10^{11}$ (3), $1\cdot10^{12}$ (4) W/m²; v_{evap}, m/sec; t, nsec.

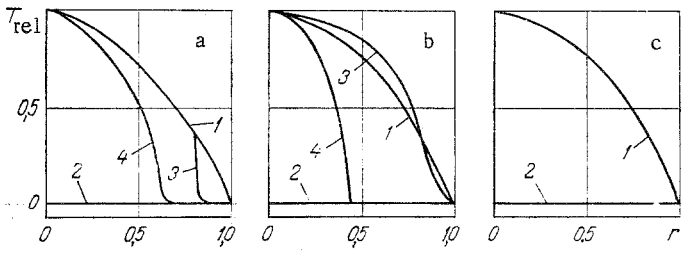

Fig. 3. Temperature distribution over particle radius at a laser radiation flux $G_0 = 5 \cdot 10^{10}$ (a), $1 \cdot 10^{11}$ (b), and $1 \cdot 10^{12}$ (c) W/m^2 ($R_0 = 9$ nm, $\tilde{\lambda} = 694.3$ nm): a) t = 20.93 (1), 21.66 (2), 21.56 (3), 21.61 (4) nsec; T = 4816 (1), 5025 (2), 4967 (3), 4981 (4) °K; b) t = 12.56 (1), 16.31 (2), 16.21 (3), 16.26 (4) nsec; T = 3161 (1), 5027 (2), 5000 (3), 5001 (4) °K; c) t = 7.65 (1), 7.75 (2) nsec; T = 4877 (1), 5060 (2) °K; T_{rel}, R, rel. units.

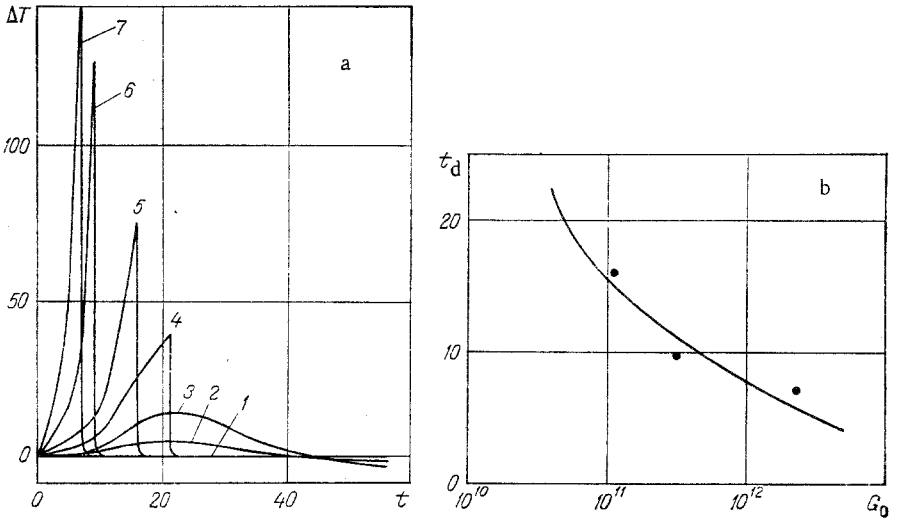

Fig. 4. Time dependence of particle radial temperature gradient (a) at laser fluxes $G_0 = 1 \cdot 10^9$ (1), $1 \cdot 10^{10}$ (2), $2.5 \cdot 10^{10}$ (3), $5 \cdot 10^{10}$ (4), $1 \cdot 10^{11}$ (5), $5 \cdot 10^{11}$ (6), $1 \cdot 10^{12}$ (7) W/m^2 and dependence of the onset of particle evaporation on G_0 (b); the points represent experimental data; $R_0 = 9$ nm, $\tilde{\lambda} = 694.3$ nm; ΔT, °K; t, t_d, nsec; G_0, W/m^2.

sorbed by the particle kG(t) and the heat-transfer coefficient. Toward the end of the pulse it is possible to observe slight cooling of the particle owing to heat emission. As the flux increases ($G_0 \geq 5 \cdot 10^{10}$ W/m^2), so does the maximum temperature and the rate of temperature change; the surface temperature reaches the sublimation point (curves 4-7), which is followed by partial (4'-5') or almost total (6'-7') destruction of the particle. The evaporation rate increases with the flux. Cooling occurs chiefly as a result of evaporation, being more intense the greater the flux and the greater the heating of the particle (curves 4-7). As compared with the previous case convective heat transfer has a less noticeable effect. This behavior has been observed experimentally [1].

Figure 1b gives the results of exposing particles with $R_0 = 5$ and 15 nm to the action of ruby laser radiation and a particle with $R_0 = 9$ nm to the action of neodymium laser radiation and its second harmonic ($\tilde{\lambda} = 530$ nm). These parameters determine the heat transfer coefficient and the dimensionless absorption coefficient.

It follows from Fig. 1b that the general behavior of T and R remains the same as in Fig. 1a. At shorter incident radiation wavelengths and a fixed initial size the heating of the particles is greater owing to the higher values of the absorption coefficient (curves 4, 1;

7, 6). For particles with different initial radii and a fixed incident radiation wavelength the heating of the particle is greater at greater R_0, since $k \sim R$, $\alpha \sim R^{-1/2}$ (curves 2, 3; 5, 8). The break on curve 5 in Fig. 1b is attributable to the fall in particle temperature toward the end of the pulse (to 5000°K or less). In this case the evaporation rate decreases sharply, and further cooling occurs as a result of heat transfer from the particle to the ambient medium.

The maximum increase in the evaporation rate is observed when the particle surface reaches a temperature of 5000°K (initial parts of curves in Fig. 2). Subsequently the rate of growth of the evaporation rate slows, although the absolute value continues to increase until the particle reaches maximum temperature values, after which it falls with fall in temperature.

Figure 3 shows the distribution of T_{rel} over r at various incident radiation fluxes for successive moments of time. At temperatures $T < 5000$°K the distribution of T_{rel} (curves 1) is similar for all the fluxes considered. At $T > 5000$°K the temperature values (2) are equalized over the radius. The reorganization of the radial distribution of the temperature field occurs when the sublimation point is reached; in this case the beginning of reorganization and its duration depend on the amount of radiation incident on the particle. As the flux increases, the reorganization of the field sets in earlier, a tendency to equalization of the temperature field is observed at lower particle temperatures, and the equalization times are sharply reduced. At $T \sim 5000$°K evaporation of the particle begins, leading to a change in many of the controlling parameters, including the dimensions of the particle, which characterize its optical properties.

At fluxes less than 10^9 W/m^2 there is practically no difference between the temperatures at the surface of and in the center of the particle. At fluxes $G_0 \approx 10^{10}$ to $2.5 \cdot 10^{10}$ W/m^2, $\Delta T \approx 10$-15°K (curves 2 and 3 in Fig. 4a), and in this case toward the end of the laser pulse the gradient may change sign, which is due to the removal of heat from the surface of the particle by forced convection prevailing over the supply of energy at the expense of the incident radiation. At greater fluxes ΔT may amount to hundreds of degrees (curves 4-7); however, when the particle surface reaches the sublimation point ΔT falls sharply to zero.

Figure 4b reveals good agreement between the time of onset of particle destruction as a function of the incident flux and the analogous values obtained from an experiment on the scattering of laser radiation by the destroyed particles.

NOTATION

k, dimensionless absorption coefficient; G_0, power density of incident radiation; Δl, distance between particles; d, particle diameter; c, ρ, λ, specific heat, density, and thermal conductivity of particle; T_0, T, R_0, R, initial and variable temperatures and radii; T_m, temperature of ambient medium; G_s, heat flux associated with energy losses through particle surface; ε, emissivity of subliming particle; σ, Stefan–Boltzmann constant; L, specific heat of vaporization; r, t, linear coordinate and time; α, heat-transfer coefficient; Nu, Nusselt number; Re, Reynolds number; λ_m, ν, thermal conductivity and kinematic viscosity of ambient medium; U, directional particle velocity; n_1, χ, refractive index and absorption coefficient of particle; ρ_1, diffraction parameter; $\tilde{\lambda}$, wavelength of incident radiation; A, atomic weight of particle material; R_g, universal gas constant; $\bar{c}$, mean velocity of sound; $\Theta = T/T^0$, $\bar{R} = R/R_0$, $\tau = t/t^0$, $\varphi = r/R_0\bar{R}(\tau)$, dimensionless temperature, radius, time, and linear coordinate; T^0, $t^0 = R_0^2/a(T_0)$, characteristic quantities; h_φ, $\Delta\tau$, difference network intervals with respect to the variables φ, τ; n, j, number of network points with respect to these variables;

$$\delta_\tau \Theta_n^j = \frac{1}{\Delta\tau}(\Theta_n^j - \Theta_n^{j-1}); \quad \Theta_{\bar{\varphi}} = \frac{1}{h_\varphi}(\Theta_n - \Theta_{n-1}); \quad \Theta_\varphi = \frac{1}{h_\varphi}(\Theta_{n+1} - \Theta_n); \quad \Theta_{\bar{\varphi},n} = \frac{1}{2}(\Theta_{\varphi,n} + \Theta_{\bar{\varphi},n}); \quad \bar{\lambda}_n = \lambda\left(\frac{\Theta_n + \Theta_{n-1}}{2}\right);$$

v_{evap}, particle evaporation rate; $T_{rel} = [T(R, t) - T(r, t)]/[T(R, t) - T(0, t)]$; $\Delta T = T(R, t) - T(0, t)$.

LITERATURE CITED

1. V. S. Burakov, V. V. Zheludok, and A. A. Stavrov, Fiz. Goreniya Vzryva, No. 2 (1974).
2. J. Reddy, Effect of Powerful Laser Radiation [Russian translation], Mir, Moscow (1974).
3. S. I. Anisimov, A. M. Bonch-Bruevich, M. A. El'yashevich, Ya. A. Imas, I. A. Pavlenko, and G. S. Romanov, Zh. Tekh. Fiz., 36, 1273 (1966).

4. Yu. V. Afanas'ev and O. N. Krokhin, Tr. Fiz. Inst. Akad. Nauk SSSR, 52, 118 (1970).
5. H. C. van de Hulst, Light Scattering by Small Particles [Russian translation], IL (1961).
6. C. Kittel, Elementary Solid State Physics, Wiley, New York (1962).
7. L. D. Landau and E. M. Lifshits, Continuum Mechanics [in Russian], GITTL, Moscow (1954), p. 253.
8. Thermodynamic Properties of Individual Substances [in Russian], Vols. 1-2, Izd. Akad. Nauk SSSR, Moscow (1962).
9. L. A. Artsimovich (editor), Nuclear Physics Handbook [Russian translation], GIFML, Moscow (1963).
10. Thermophysical Properties of Solids [in Russian], Nauka, Moscow (1973).
11. D. Ya. Svet, Objective Methods of High-Temperature Pyrometry for a Continuous Radiation Spectrum [in Russian], Nauka, Moscow (1968).
12. Yu. K. Krylov, Questions of Quantum Electronics. Transactions of the Leningrad Institute of Precision Mechanics and Optics, [in Russian], No. 65, Leningrad (1968), p. 55.
13. N. B. Vargaftik, Handbook of Thermophysical Properties of Gases and Liquids [in Russian], Nauka, Moscow (1972).
14. A. G. Blokh, Thermal Radiation in Boilers [in Russian], Énergiya, Leningrad (1967).
15. V. R. Stull and G. N. Plass, J. Opt. Soc. Amer., No. 2 (1960).
16. I. P. Dobrovol'skii and A. A. Uglov, Kvant. Elektron., 1, 1423 (1974).
17. S. I. Anisimov, Ya. A. Imas, G. S. Romanov, and Yu. V. Khodyko, Effect of High-Power Radiation on Metals [in Russian], Nauka, Moscow (1970), p. 97.
18. O. Knake and I. N. Stranskii, Usp. Fiz. Nauk, 68, 261 (1959).
19. R. J. Thorn and G. H. Winslow, J. Chem. Phys., 26, 186 (1957).
20. A. A. Samarskii, Introduction to the Theory of Difference Schemes [in Russian], Nauka, Moscow (1971).
21. A. A. Samarskii, Zh. Vychisl. Mat. Mat. Fiz., 2, No. 5 (1962).
22. I. V. Fryazinov and M. I. Bakirova, Zh. Vychisl. Mat. Mat. Fiz., 12, No. 2 (1972).
23. R. D. Richtmyer and K. W. Morton, Difference Methods for Initial-Value Problems, 2nd ed., Wiley (1967).
24. I. S. Berezin and N. P. Zhidkov, Computational Techniques [in Russian], Vol. 1, Fizmatgiz, Moscow (1959), p. 77.
25. O. A. Oleinik, Dokl. Akad. Nauk SSSR, 135, No. 5 (1960).

NUMERICAL METHOD FOR THE SOLUTION OF PROBLEMS OF NONSTEADY NONLINEAR THERMAL CONDUCTION OF COMPLEX TWO-DIMENSIONAL BODIES

G. K. Malikov

UDC 536.24.02

The method involves the use of a nonrectangular orthogonal grid, the form of which is determined by the boundary of the body; a single calculation algorithm suitable for bodies of various shapes is obtained.

Using the well-known finite-difference method [1], it is difficult to construct a single algorithm for the temperature field of two-dimensional bodies of various shapes; this is because a rectangular grid, as a rule, provides a poor fit to the boundaries of the body and requires individual programming for each body.

In physical terms, the essence of the phenomenon is that heat fluxes flow from the boundary into the body and meet at centers or lines of symmetry of the body; accordingly, consider a system of coordinate lines y in the form of straight lines from the boundary running

All-Union Scientific-Research Institute of Metallurgical Thermoengineering, Sverdlovsk.
Translated from Inzhenerno-Fizicheskii Zhurnal, Vol. 32, No. 5, pp. 905-912, May, 1977. Original article submitted May 13, 1976.